Reducing contact forces in the arch and supra-aortic vessels using the Magellan robot

Hedyeh Rafii-Tari, MASc,[a] **Celia V. Riga, MD, FRCS,**[b,c] **Christopher J. Payne, MEng,**[a] **Mohamad S. Hamady, FRCR,**[c] **Nicholas J. W. Cheshire, MD, FRCS,**[b,c] **Colin D. Bicknell, MD, FRCS,**[b,c] and **Guang-Zhong Yang, PhD, FREng,**[a] *London, United Kingdom*

Objective: **Conventional catheter manipulation in the arch and supra-aortic trunks carries a risk of cerebral embolization. This study proposes a platform for detailed quantitative analysis of contact forces (CF) exerted on the vasculature, in order to investigate the potential advantages of robotic navigation.**

Methods: **An anthropomorphic phantom representing a type I bovine arch was mounted and coupled onto a force/torque sensor. Three-axis force readings provided an average root-mean-square modulus, indicating the total forces exerted on the phantom. Each of the left subclavian, left common carotid, and right common carotid arteries was cannulated within a simulated endovascular suite with conventional (n = 42) vs robotic techniques (n = 30) by two operator groups: experts and novices. The procedure path was divided into three phases, and performance metrics corresponding to mean and maximum forces, force impact over time, standard deviation of forces, and number of significant catheter contacts with the arterial wall were extracted.**

Results: **Overall, median CF were reduced from 1.20 N (interquartile range [IQR], 0.98-1.56 N) to 0.31 N (IQR, 0.26-0.40 N; $P < .001$) for the right common carotid artery; 1.59 N (IQR, 1.11-1.85 N) to 0.33 N (IQR, 0.29-0.43 N; $P < .001$) for the left common carotid artery; and 0.84 N (IQR, 0.47-1.08 N) to 0.10 N (IQR, 0.07-0.17 N; $P < .001$) for the left subclavian artery. Robotic navigation resulted in significant reductions for the mean and maximum forces for each procedural phase. Significant improvements were also seen in other metrics, particularly at the target vessel ostium and for the more anatomically challenging procedural phases. Force reductions using robotic technology were evident for both novice and expert groups.**

Conclusions: **Robotic navigation can potentially reduce CF and catheter-tissue contact points in an in vitro model, by enhancing catheter stability and control during endovascular manipulation. (J Vasc Surg 2016;64:1422-32.)**

Clinical Relevance: **Cerebral embolization and the risk of stroke remain as major concerns in advanced endovascular interventions in the aortic arch. Steerable robotic catheter navigation has the potential to reduce the embolic burden by reducing contact forces and catheter-tissue contact during different phases of arch navigation and carotid cannulation, with implications on improved training and reduced learning curves for complex endovascular procedures in the clinical setting.**

Cardiovascular disease remains the major cause of mortality in the western world, with stroke being the third leading cause of death as well as the leading cause for serious and long-term disability.[1] The effectiveness of carotid artery stenting (CAS) in the prevention of stroke remains controversial, with most randomized controlled trials demonstrating higher periprocedural rates of stroke and death compared with carotid endarterectomy (CEA).[2,3] Despite improved patient selection, increased operator experience, and advances in stent and embolic protection device technology, the intraprocedural risk of stroke is still a concern with a 61% relative risk increase of periprocedural stroke or death compared with CEA.[4] The embolic burden reported in magnetic resonance diffusion-weighted imaging (DWI) studies reaches 30% to 50%,[5-7] and although these DWI lesions may not be clinically overt, they represent the overall thromboembolic risk of endovascular carotid intervention. Furthermore, DWI coupled with transcranial Doppler monitoring has demonstrated that cerebral

From The Hamlyn Centre for Robotic Surgery,[a] Academic Division of Surgery,[b] Imperial College London, and the Imperial Vascular Unit, St. Mary's Hospital.[c]

This study was supported in part by the Institute of Global Health Innovation, Imperial College NIHR Biomedical Research Centre, and the Wates Foundation.

Author conflict of interest: Institution-level research support was received from Hansen Medical. C.V.R. is a consultant for Hansen Medical.

Presented as a poster at the Twenty-eighth Annual Meeting of the European Society for Vascular Surgery, Stockholm, Sweden, September 23-26, 2014.

Correspondence: Celia V. Riga, MD, FRCS, Department of Biosurgery and Surgical Technology, 10th Flr QEQM Bldg, St. Mary's Hospital, Praed St. London, W2 1NY, UK (e-mail: c.riga@imperial.ac.uk).

The editors and reviewers of this article have no relevant financial relationships to disclose per the JVS policy that requires reviewers to decline review of any manuscript for which they may have a conflict of interest.

0741-5214

http://dx.doi.org/10.1016/j.jvs.2015.06.215

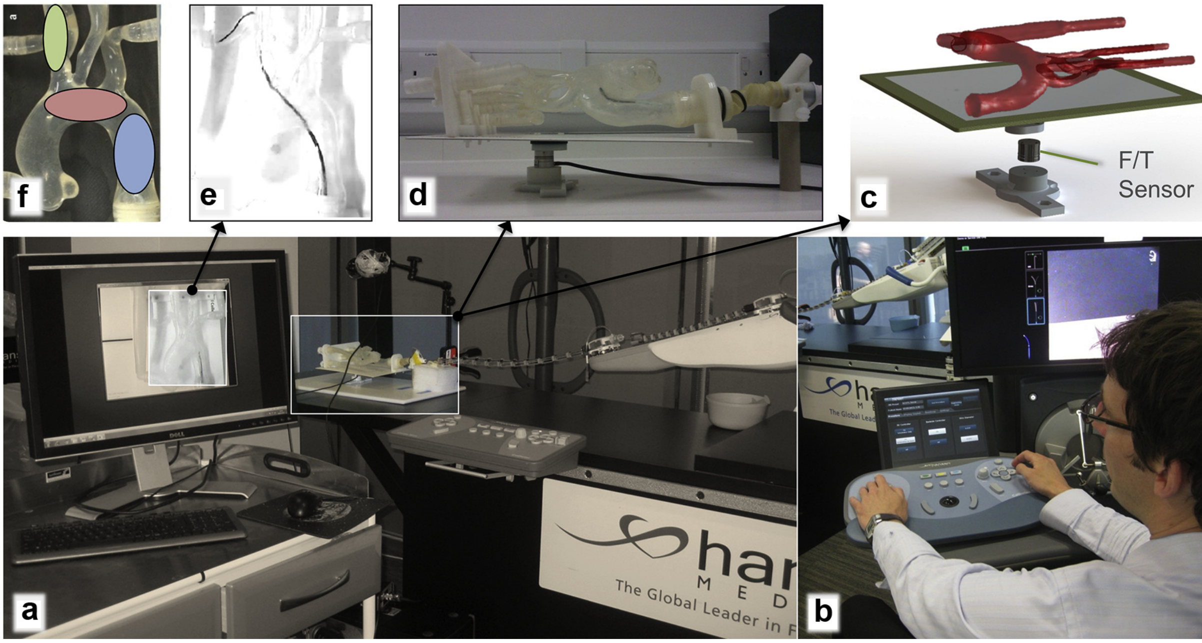

Fig 1. Experimental setup depicting the robotic catheter **(a)**, the operator workstation **(b)**, detailed view of the force measurement platform and force/torque (*F/T*) sensor **(c** and **d)**, simulated fluoroscopy image for guidance **(e)**, and the three procedural phases **(f)**.

protection both with proximal and distal devices significantly reduces distal embolization both for the ipsilateral as well as the contralateral carotid territories.[7-11] A high number of isolated microemboli specifically during wire and catheter manipulations has been reported, highlighting the importance of cannulation techniques.[12-14] These findings suggest that one of the determinants of thromboembolic events in CAS relates to instrumentation of the aortic arch and proximal supra-aortic trunks as well as instability during carotid lesion crossing. The risk of embolization has also been highlighted for other procedures that involve endovascular manipulation and use of endovascular tools in the aortic arch, such as transfemoral aortic valve replacement (TAVI) and thoracic endovascular aortic repair (TEVAR).[15-18] Factors that relate to the biomechanical properties of endovascular manipulation tools and operator skill have not been properly evaluated in any trial.

Although increasingly becoming a necessity in electrophysiology procedures,[19,20] information on tool-tissue interactions in the peripheral vasculature is limited. Quantification of the contact forces (CF) resulting from interactions between catheters, guidewires, and other endovascular devices within the vasculature itself can provide important insights into potential intraprocedural risks. The CAS trial results to date have prompted alternative approaches focusing on transcervical access routes, arch avoidance, and flow reversal techniques.[21,22] Robotically steerable catheter navigation systems have enjoyed a growing interest in recent years,[23] and have demonstrated potential advantages in preclinical studies in terms of cannulation efficiency, catheter tip movements, and stability during wire exchanges during CAS.[24-26] This study investigates the potential advantages of robotic navigation by proposing a platform within a simulated framework for detailed and quantitative analysis of forces exerted during arch manipulation, in order to understand the role of intelligent catheter systems in minimizing risk and increasing procedural efficiency.

METHODS

The Magellan robotic system. The development of the next-generation Magellan system (Hansen Medical, Mountain View, Calif) was based on the original Sensei X platform—originally designed for transvenous cardiac mapping and ablation procedures—but with significant modifications and has been described in past publications.[27] In brief, it is an electromechanical master-slave system, consisting of the operator's workstation and the remote catheter manipulator (robotic arm), which delivers the steerable robotic catheter (Fig 1, *a*). The robotic catheter consists of an inner leader (inner diameter 3 Fr; outer diameter 6 Fr) within an outer sheath (inner diameter 6 Fr; outer diameter 9 Fr), and six-degree-of-freedom control of both sheath and leader is enabled via four pull-wires drivers with maximum articulation angles of 180° and 90° respectively. The system offers full rotational ability and a leader workspace defined by a bend of up to 180° and a 21 cm extension, and, more importantly, independent torque control at the tip without catheter shaft rotation. Furthermore, a robotic wire manipulator allows remote insertion, rotation, and retraction of conventional 0.018″ and 0.035″ hydrophilic wires. The mobile workstation incorporates the master controller, the

Table I. Median values for statistically significant differences (Mann-Whitney *U* test; $P < .05$) between metrics for robotic (n = 30) vs manual (n = 42) cannulation of the right common carotid artery (*RCCA*), left common carotid artery (*LCCA*), and left subclavian artery (*LSA*), at each of the three phases of the procedure

	Descending aorta			*Aortic arch*			*Arch vessel*		
	P	*Robotic*	*Manual*	P	*Robotic*	*Manual*	P	*Robotic*	*Manual*
RCCA									
Maximum force, N	<.001	**0.05**	0.25	<.001	**0.25**	0.78	<.001	**0.29**	1.19
FIT, N.s	.045	0.43	0.68	NS	–	–	<.001	**1.17**	2.95
STDEV, N	<.001	**0.01**	0.05	<.001	**0.05**	0.18	<.001	**0.04**	0.23
# peaks	.043	0.5	2.1	.023	0	10	.001	**0**	9.5
Mean force, N	<.001	**0**	0.16	<.001	**0.15**	0.30	<.001	**0.21**	0.31
LCCA									
Maximum force, N	<.001	**0.05**	0.22	<.001	**0.19**	0.68	<.001	**0.32**	1.59
FIT, N.s	NS	–	–	NS	–	–	<.001	**1.62**	7.92
STDEV, N	<.001	**0.01**	0.04	<.001	**0.03**	0.13	<.001	**0.05**	0.33
# peaks	NS	–	–	<.001	**0**	8	<.001	**1**	30
Mean force, N	<.001	**0**	0.14	<.001	**0.14**	0.25	<.001	**0.21**	0.37
LSA									
Maximum force, N	<.001	**0.06**	0.20	<.001	**0.06**	0.27	<.001	**0.08**	0.83
FIT, N.s	.004	0.36	0.73	.004	0.16	0.56	<.001	**0.24**	1.30
STDEV, N	<.001	**0.02**	0.04	<.001	**0.004**	0.54	<.001	**0.01**	0.17
# peaks	NS	–	–	<.001	**0**	4	<.001	**0**	5
Mean force, N	<.001	**0**	0.14	<.001	**0**	0.18	<.001	**0**	0.27

FIT, Force impact over time; *NS,* not statistically significant; *STDEV,* standard deviation.
Metrics with $P < .001$ have been highlighted in bold.

three-dimensional hand-operated joystick with seven degrees of freedom, and the display screens, and is situated away from x-ray radiation, as shown in Fig 1, *b*.

Force measurement platform and experimental setup. A silicone-based, transparent, anthropomorphic phantom (Elastrat Sarl, Geneva, Switzerland), representing a type I aortic arch with bovine configuration of the left common carotid artery (LCCA) was used. The phantom was mounted onto a platform and rigidly coupled to a six-axis force-torque (F/T) sensor (Nano17; ATI Industrial Automation, Inc, Apex, NC), providing force and torque readings in each of the three (X, Y, and Z) directions. The platform was developed to provide accurate and direct measurement of the forces exerted on the vasculature (Fig 1, *c*). From the three-axis force measurements obtained from the sensor, an average root-mean-square force modulus was calculated, indicating the total forces exerted on the vascular model. The catheter was inserted through a custom-made introducer sheath and flexible section of tubing before entering the phantom. The introducer sheath was isolated and decoupled from the force measurement platform, so that only local force measurements corresponding to direct catheter-vessel contact were measured, without the friction in the introducer sheath contaminating the measurements (Fig 1, *d*). A camera was mounted above the phantom, with the video feed projected onto a monitor to be used by operators for navigation. In order to simulate 2D fluoroscopy guidance, the live images obtained from the camera were processed using contrast, brightness, and color adjustments, to remove the contours of the vessels and prevent depth perception while still allowing visualization of the catheter and guidewire (Fig 1, *e*).

Acquisition and synchronization of the video feed and force data was achieved by custom software created in C++ to record the force data through LabVIEW (National Instruments Corp, Austin, Tex), and the OpenCV (Open Source Computer Vision) library for processing, displaying, and recording the video feed. The F/T sensor transmits data at a frequency of 25 Hz, and is able to detect forces to a resolution of 4 milli-Newtons (mN). The F/T sensor was zeroed in order to omit the weight of the phantom and platform, and re-zeroed at the beginning of data collection for each individual run, to ensure that the force readings represent only the CF between the catheter/guidewire and the vascular phantom.

Study protocol. Conventional arch vessel cannulation was performed by 14 operators of varying endovascular experience (four experienced endovascular specialists who had performed >300 endovascular procedures and 10 novice operators who had performed <10 endovascular procedures). All procedures were performed using the same Terumo wire and a conventional 5F-shaped catheter. Each operator was asked to cannulate the supra-aortic vessels, namely the left subclavian artery (LSA), the LCCA, and the right common carotid artery (RCCA) three times in a randomized order, resulting in a total of 42 cannulations for each target vessel across the expert (n = 12) and novice (n = 30) operator groups. Vessel cannulation using the robotic platform was performed by seven operators of varying experience (two endovascular specialists with previous Magellan experience, as well as five novice operators with no previous experience in using the robotic platform). Robotic cannulations were performed using a Terumo wire and the robotic catheter (consisting of

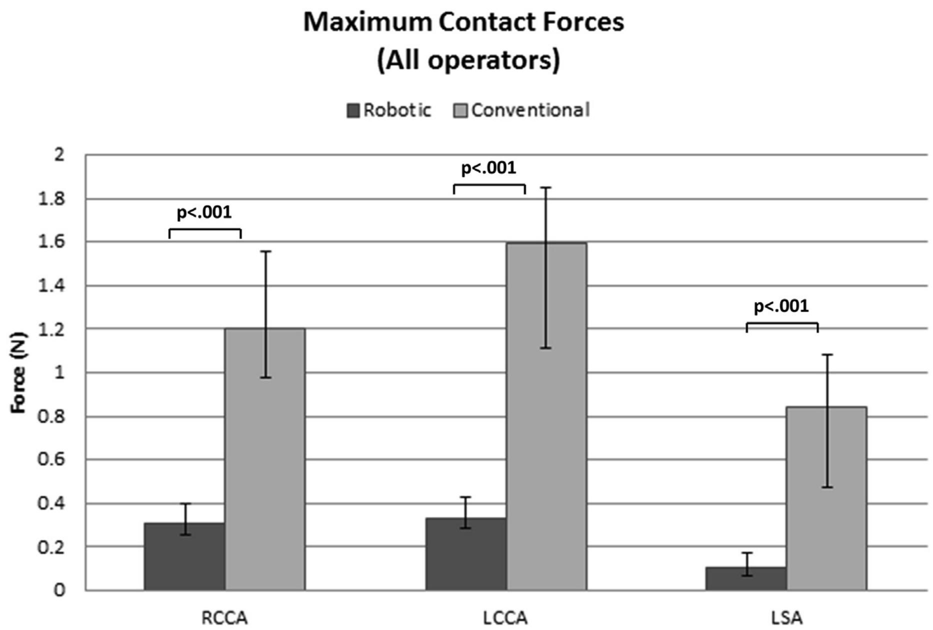

Fig 2. Bar chart shows the median values for the maximum contact forces (CF) exerted during cannulation of each of the arteries for the robotic vs the manual approach, across all operators. The *error bars* represent the interquartile ranges (IQRs; Wilcoxon rank test). *LCCA,* Left common carotid artery; *LSA,* left subclavian artery; *RCCA,* right common carotid artery.

the inner "leader" within the outer "sheath") without the use of any conventional catheters. Novice operators underwent a short teaching session followed by a practical demonstration on the robotic system before commencing the study. Each target vessel was cannulated 30 times in a randomized order across the experienced (n = 15) and novice (n = 15) operator groups.

Data analysis. The procedure path for each target vessel was divided into three phases: (1) advancement of wire/catheter in the descending aorta; (2) navigating the aortic arch; and (3) cannulation of the arch vessel. These procedural phases are displayed in Fig 1, *f*. The force measurements recorded for each run were postprocessed to remove any force bias, by subtracting all forces from the minimum recorded force value of that procedure, corresponding to no tool-tissue interaction. Different performance metrics were then extracted for each of the three phases of the procedure. These metrics include: maximum force value (N); force impact over time (FIT; N.s), calculated by measuring the area under the force signals (corresponding to the force-time integral); standard deviation of forces (N); number of force peaks, which was chosen to correspond to the number of significant contacts between the catheter and the arterial wall above a threshold of 0.3 N, calculated by finding the local maxima in the force signal above that threshold; mean force (N), which was calculated for forces larger than 0.1 N, in order to be above the noise ceiling of the sensor and restrict data to tool-tissue interactions while preventing task delays from affecting the mean force assigned to a trial. All data processing and statistical analysis were performed with the Matlab software (The MathWorks Inc, Natick, Mass). Differences between robotic and manual performance were assessed using the nonparametric significance tests. A value of $P < .05$ was considered statistically significant.

RESULTS

Robotic navigation resulted in significant reductions for mean and maximum forces for each procedural phase and for all targets. Table I shows differences in performance metrics between robotic vs manual vessel cannulation for the RCCA, LCCA, and LSA, respectively, depicting the values for statistically significant differences during each procedural phase. Significant improvements can also be seen in the other metrics, particularly at the target vessel ostium, and for the more anatomically challenging procedural phases. CF were reduced from 1.20 N with an interquartile range (IQR) of 0.98-1.56 N to 0.31 N (IQR, 0.26-0.40 N; $P < .001$) for the RCCA; 1.59 N (IQR, 1.11-1.85 N) to 0.33 N (IQR, 0.29-0.43 N; $P < .001$) for the LCCA; and 0.84 N (IQR, 0.47-1.08 N) to 0.10 N (IQR, 0.07-0.17 N; $P < .001$) for the LSA (Fig 2). Force reductions using robotic technology were evident for both novice and expert groups.

Fig 3 illustrates the differences between manual and robotic techniques using RCCA cannulation as an example of the forces measured over time, for an expert (Fig 3, *a*) and novice (Fig 3, *b*) operator. The three colors depict the three distinct procedural phases, whereas the lighter and darker colors demonstrate conventional vs robotic navigation techniques respectively. These graphs highlight the significantly lower force values seen during robotic manipulation. For the expert operator, the robotic approach takes longer than the manual technique; however, the forces

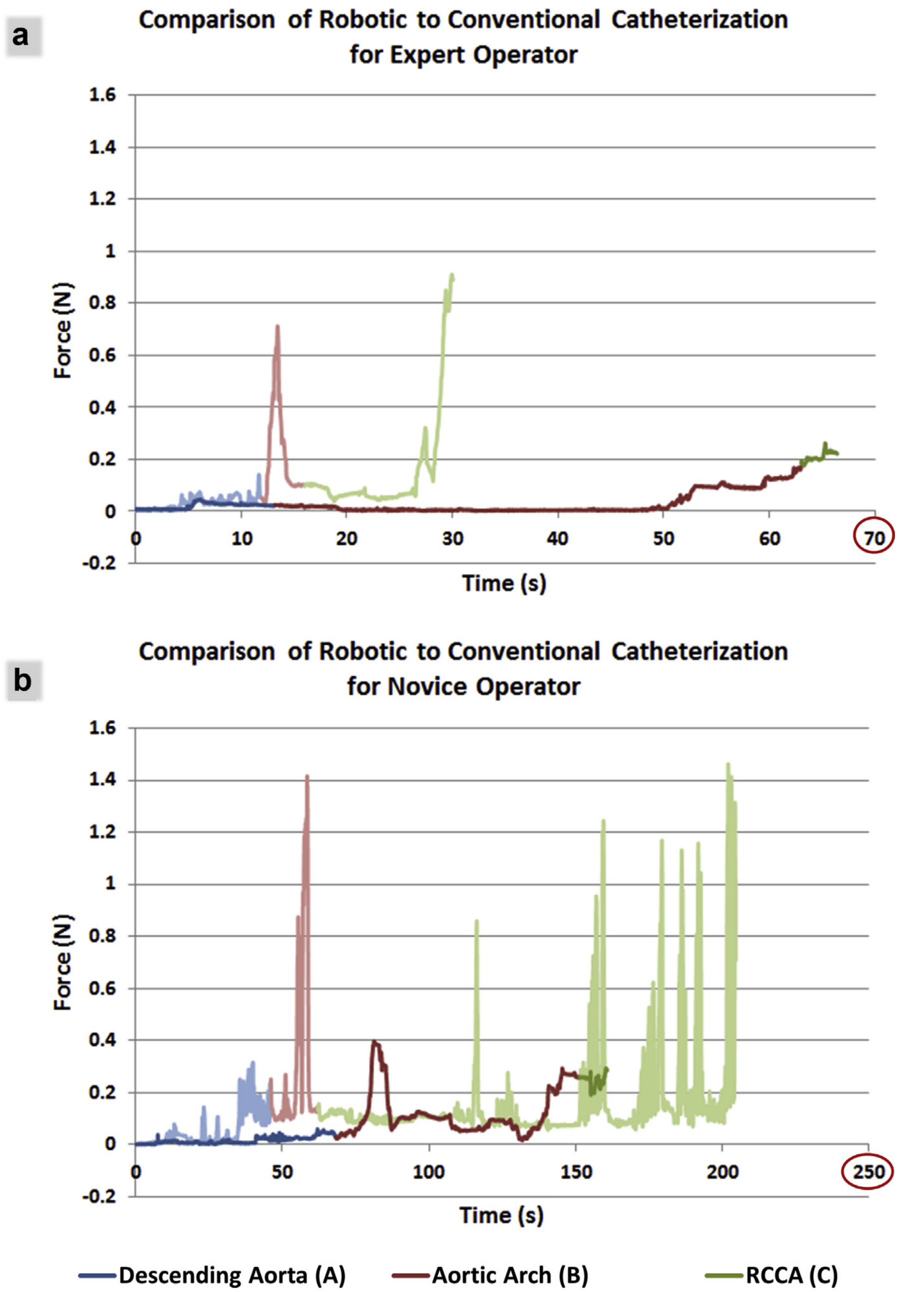

Fig 3. Examples of contact forces (CF) exerted by expert **(a)** and novice **(b)** operators, with the conventional (*light color*) and robotic (*dark color*) approach. The colors show the three phases of the procedure for cannulation of the right common carotid artery (*RCCA*).

particularly over the aortic arch and at the target vessel ostium are significantly reduced. For the novice operator, the robotic approach significantly improves the performance both in terms of cannulation speed as well as the magnitude of forces exerted on the vasculature. This is more noticeable during manipulation near the supra-aortic trunks and target vessel ostium.

Fig 4 depicts the catheter path within a mesh of the vascular phantom during cannulation of the same RCCA, for the manual (Fig 4, *a*) vs the robotic (Fig 4, *b*) approach, performed by an expert operator. The color gradient depicts the magnitude of the force applied on the vascular model over the catheter path, which is notably lower using the Magellan robot.

The number of significant contacts on the aortic arch wall was also significantly reduced with the robotic catheter system, irrespective of the endovascular experience of the operator. The median number of contacts were reduced from 8 to 0 ($P = .017$) for the LSA, from 37 to 3.5

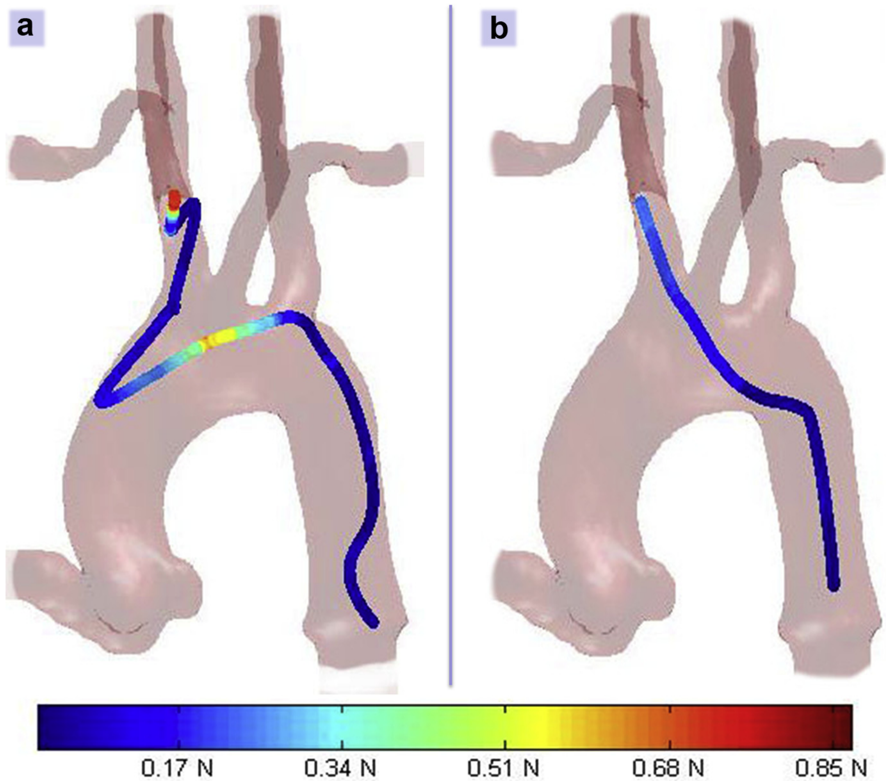

Fig 4. Color gradient depicting the magnitude of the contact forces (CF) over the catheter path for the manual **(a)** vs robotic **(b)** approach, for cannulation of the right common carotid artery (RCCA) by an expert operator.

(P <.001) for the LCCA, and from 21 to 1 (P <.001) for the RCCA (Fig 5, *a*). Median values for FIT (in N.s) and for all the operators were also reduced from 3.52 (IQR, 1.41-5.48) to 0.80 (IQR, 0.56-1.44; P < .001) for successful cannulation of the LSA, from 9.66 (IQR, 6.64-13.60) to 4.88 (IQR, 2.43-9.89; P = .007) for the LCCA, and from 6.11 (IQR, 4.59-8.24) to 4.16 (IQR, 2.36-9.73; P = .29), as shown in Fig 5, *b*.

Table II shows the percentage improvements in the average maximum force and average mean force values for robotic catheterization as compared with conventional catheterization for each experience group. The results compare the improvements between expert operators and novice operators at each procedural phase for cannulation of each of the RCCA, LCCA, and LSA. As shown, the novice group has a higher percentage of improvement with the robotic technology, as compared with the expert group.

DISCUSSION

Endovascular intervention in the arch and supra-aortic trunks is associated with a risk of cerebral embolization not only during carotid intervention but also during other procedures that involve endovascular manipulation in the aortic arch such as TAVI and TEVAR.[2-4,15-18] Compared with patients undergoing CEA, patients treated with CAS have higher numbers of periprocedural ischemic brain lesions, which on DW-MRI are smaller and more likely to occur in cortical areas and subjacent white matter.[4] A significant number of these new lesions (25%-45%) are found in other vascular territories, including the contralateral hemisphere,[10,13,17] suggesting that they arise from an atherosclerotic aortic arch and arch vessels during the manipulation of endoluminal devices. Use of a coaxial system, similar to the robotic system, has been shown to significantly reduce the incidence of new ischemic lesions on DWI in other territories.[13] Furthermore, there is DWI and transcranial Doppler evidence that cerebral protection significantly reduces the distal embolization rate both ipsilateral and contralateral carotid territories.[7-11] A significant number of isolated microemboli specifically during wire and catheter manipulations has also been reported, both in CAS and TEVAR, highlighting the importance of cannulation techniques.[12-14,18] In an analysis of 627 protected CAS procedures, Verzini et al documented 10 major strokes, four of which occurred during the cannulation phase involving the arch vessel origin or the CCA itself.[14]

Factors that can contribute to difficulties and increase the risk of procedural embolization include complex arch anatomy, carotid plaque morphology, and operator experience.[5] Most of these factors coupled with conventional catheter instability increase the potential for prolonged instrumentation in the arch and CCA origins. Consequently, alternative approaches have recently emerged focusing on arch avoidance and controlled blood-flow reversal techniques.[21,22]

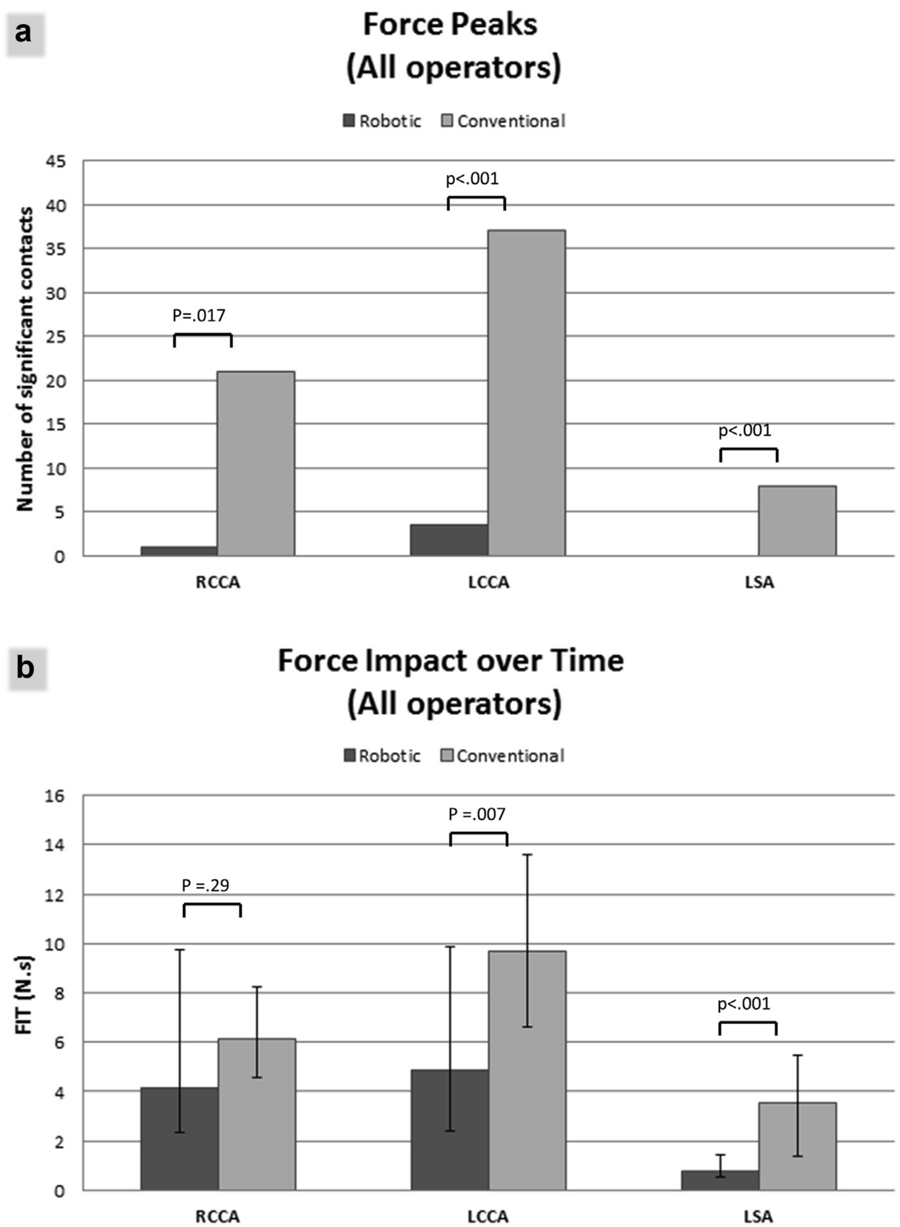

Fig 5. Bar charts show the median values for the number of force peaks (significant contacts) with the aortic arch wall during cannulation of each of the arteries for the robotic vs the manual approach **(a)**, as well as the median values for the force impact over time (*FIT*) during cannulation of each of the arteries for the robotic vs the manual approach **(b)**, across all operators. The *error bars* represent the interquartile ranges (IQRs; Wilcoxon rank test). *LCCA,* Left common carotid artery; *LSA,* left subclavian artery; *RCCA,* right common carotid artery.

Endovascular robotic technology, despite its widespread use in electrophysiology,[28] is a comparatively new field of work in catheter-based arterial intervention; nonetheless, interest and clinical experience are growing.[24,27,29-31] Previous comparative in vitro studies analyzing 272 arch vessel cannulations performed by multiple operators of varying endovascular experience highlighted the potential advantages of robotic navigation with faster access to target times, shorter navigation paths, reduced number of vessel wall hits and catheter movements, and improved catheter stability during wire exchanges.[25,26,32] The majority of these studies have relied on video-based assessment and qualitative rating scales. The direct, biomechanical effects of robotic as well as conventional catheter interactions with the vasculature, however, have not been quantitatively evaluated and currently remain unknown. Animal studies have previously reported histological evidence of reduced instrumentation suggestive of reduced vessel wall interactions for robotic

Table II. Percentage improvements for expert and novice performance from conventional (expert, n = 12; novice, n = 30) to robotic (expert, n = 15; novice, n = 15) catheterization in average mean force and average maximum force at each procedural phase for cannulation of each artery

	Descending aorta		*Aortic arch*		*RCCA*	
	Experts	*Novices*	*Expert*	*Novice*	*Expert*	*Novice*
Average maximum force, %	49.4	83.1	63.2	70.3	55.7	80.3
Average mean force, %	45.2	99.9	50.1	46.4	2.6	40.6
	Descending aorta		*Aortic arch*		*LCCA*	
	Expert	*Novice*	*Expert*	*Novice*	*Expert*	*Novice*
Average maximum force, %	43.2	81.7	65.3	65.0	40.3	80.0
Average mean force, %	46.5	99.9	48.0	41.0	0.0	54.2
	Descending aorta		*Aortic arch*		*LSA*	
	Expert	*Novice*	*Expert*	*Novice*	*Expert*	*Novice*
Average maximum force, %	57.0	76.9	79.2	82.2	81.7	88.9
Average mean force, %	53.2	94.6	76.2	92.4	78.8	83.2

LCCA, Left common carotid artery; *LSA,* left subclavian artery; *RCCA,* right common carotid artery.

navigation.[33,34] Direct measurement of CF on the vasculature, however, is novel for peripheral vascular interventions and may provide important insights on the current state of robotic catheter navigation systems, and their potential advantages compared with conventional techniques.

The study of force feedback and information on tool-tissue interactions to prevent tissue trauma during manipulation as well as successful training and simulation, has received attention in the field of laparoscopic minimally invasive surgery. Different studies in laparoscopic surgery have evaluated the use of force-sensing platforms for providing adjunctive force-related information towards training and assessment of surgical skill, as well as comparing robotic technology with conventional cardiac surgery on ex vivo animal models using the da Vinci Surgical System (Intuitive Surgical, Inc, Sunnyvale, Calif).[35,36] A key trend in recent years in cardiac electrophysiology is the incorporation of force-sensing technologies for measuring CF at the catheter tip such as in the TactiCath catheter (Endosense SA, Geneva, Switzerland) and the IntelliSense Sensei X (Hansen Medical, Mountain View, Calif). These devices are designed to avoid excessive forces as well as maintain good contact between catheter electrodes and the myocardial wall for cardiac ablation.[37-39] For peripheral vascular procedures, different studies have attempted to show the significance of haptic cues that are felt by operators during conventional catheter navigation, and the advantage of providing additional force feedback towards reducing potential intraprocedural risks in the aortic arch.[40,41] However, no established commercial force-sensing solutions exist as of yet, and no quantitative metrics related to tool-tissue interactions have been studied in depth in the past.

In existing commercial robotic systems such as the Magellan, the lack of force-sensing and haptic feedback prevents the transmission of catheter-tissue interaction forces and haptic cues that would be felt by the operators during the conventional technique. Catheter force-sensing technologies for peripheral vascular procedures still remain in the research stage due to miniaturization problems associated with the smaller size of the catheters. Furthermore, the need for measuring not just tip but also side forces resulting from the interaction of the entire catheter shape with the vasculature remains unresolved. Proximal force-sensing of the catheters is a potential solution; however, this method cannot distinguish between friction in the introducer sheath and collisions between the catheter and vasculature. Therefore, the effects of robotic catheter interactions with the anatomy, as compared with the manual techniques, have so far been unknown.

The data from this study offers significant insights into the forces exerted on the vasculature during endovascular manipulation in the arch and supra-aortic trunks, while depicting significant improvements in the mean and maximum forces, FIT, and number of catheter contacts, with robot-assisted navigation over the conventional approach. The results demonstrate significant improvements for all metrics (mean and maximum forces, FIT, standard deviation of forces, number of significant contacts) with the robotic approach, for the different procedural phases as well as cannulation of different target arch vessels. The maximum exerted force by the robotic system is significantly lower for all three phases of the procedure and for all three arteries. The FIT shows significant improvements with the robotic approach, particularly during the cannulation phase at the ostium of the artery.

The standard deviations of the forces are also significantly lower for all three phases of the procedure, indicating a more continuous, repeatable, and stable contact with the vasculature for the robotic catheter. The number of significant contacts with the vessel walls are also significantly reduced with the robotic approach, particularly for the more complex parts of the anatomy (navigating around the arch and targeting the vessel ostium). This is more evident during cannulation of the LCCA, which, in this experimental model, was the most anatomically challenging vessel due to its bovine configuration. Mean forces are reduced to a median of zero for all phases when cannulating the LSA and when advancing through the descending aorta for the LCCA and RCCA, and are also significantly lower for the next two phases of the procedure. Reduced magnitude and time impact of the forces, as well as a reduction in vessel wall contacts for the robotic catheter, are indicators of the increased safety and enhanced catheter stability provided by the robotic catheter, as well as more controlled vessel centerline navigation capabilities of this technique, which may potentially reduce the risk of embolization and stroke. These improvements may further be attributed to elimination of tremor and added operator comfort by enabling the operator to perform the procedure in a seated position with the robotic technology.

Numerous studies have highlighted the steep learning curves associated with safe CCA cannulation and successful CAS outcomes, which are highly dependent on operator experience.[5,6,42] The results of our study suggest that, despite the short training time of the operators on the robotic platform, significant improvements were observed in the average mean and maximum forces exerted during the cannulation with the robotic technique, irrespective of the operator's endovascular experience. Higher percentage improvements were seen for the novice group, as compared with the expert cohort, showing the potential of robotic catheterization in reducing the steep learning curves associated with these procedures as highlighted in previous reports.[43] These findings highlight the ease of use and intuitive nature of robotic technology, with important implications towards clinical adoption and training.

Clinical assessment of endovascular skill has thus far relied mainly on qualitative global rating scales, time-action analysis, and virtual reality simulators.[44,45] However, endovascular skill evaluation suffers from a lack of objective quantitative skill assessment measures, as commercially available simulators do not take into account the biomechanical properties of manipulation, the devices, and the vasculature itself. Very few studies have looked at operator motion patterns and biomechanical and behavioral data.[40,46,47] A realistic simulation environment that enables accurate, quantitative, and objective measurements of manipulation patterns, operator tool interactions, and forces exerted on the vasculature can significantly improve training and assessment of endovascular skill.[48]

The work presented constitutes a pilot study conducted by a small cohort of experienced and novice operators to validate the feasibility of the proposed force-sensing platform in studying the potential advantages of robotic catheter technology. Future work will include a larger pool of endovascular specialists to further evaluate its use. Furthermore, the use of in vitro phantoms has inherent limitations by not reflecting the mechanical properties of real tissue and all the clinical challenges associated with catheter navigation in an atherosclerotic arch. Further studies with ex vivo porcine as well as cadaver tissue are encouraged with the proposed platform, to provide more realistic biomechanical properties and tool-tissue interactions. This may also have further implications for TAVI[49] and other invasive cardiology procedures, as well as neurointervention.

CONCLUSIONS

Conventional endovascular manipulation in the arch is associated with a high risk of cerebral embolization and stroke. The results in this study demonstrate the potential of steerable robotic catheter navigation in reducing the CF and catheter tissue contact during different phases of arch navigation and carotid cannulation, by enhancing catheter stability as well as improved accuracy and control. The results also suggest ease of use for robotic technology irrespective of the operator's experience level, with implications towards reduced learning curves and clinical adoption. The proposed platform and F/T sensor can be used to understand the role of endovascular tools to minimize risk and increase procedural efficiency, with further applications towards objective and quantitative training and assessment of endovascular skill.

AUTHOR CONTRIBUTIONS

Conception and design: HR, CR, CP, NC, CB, GY
Analysis and interpretation: HR, CR, CP, CB
Data collection: HR, CR, CP, MH, NC, CB
Writing the article: HR, CR, CP, CB, GY
Critical revision of the article: HR, CR, CP, MH, NC, CB, GY
Final approval of the article: CR, GY
Statistical analysis: HR, CR
Obtained funding: CR, GY
Overall responsibility: GY
HR and CR contributed equally to this article and share co-first authorship.

REFERENCES

1. Lloyd-Jones D, Adams RJ, Brown TM, Carnethon M, Dai S, De Simone G, et al. Executive summary: heart disease and stroke statistics—2010 update: a report from the American Heart Association. Circulation 2010;121:948-54.
2. Mantese VA, Timaran CH, Chiu D, Begg RJ, Brott TG. The carotid revascularization endarterectomy versus stenting trial (CREST) stenting versus carotid endarterectomy for carotid disease. Stroke 2010;41(10 Suppl 1):S31-4.
3. Ederle J, Featherstone RL, Brown MM. Randomized controlled trials comparing endarterectomy and endovascular treatment for carotid artery stenosis: a Cochrane systematic review. Stroke 2009;40:1373-80.
4. Kakisis J, Avgerinos E, Antonopoulos C, Giannakopoulos T, Moulakakis K, Liapis C. The European Society for Vascular Surgery

guidelines for carotid intervention: an updated independent assessment and literature review. Eur J Vasc Endovasc Surg 2012;44:238-43.
5. Gensicke H, Zumbrunn T, Jongen LM, Nederkoorn PJ, Macdonald S, Gaines PA, et al. Characteristics of ischemic brain lesions after stenting or endarterectomy for symptomatic carotid artery stenosis: results from the International Carotid Stenting Study—Magnetic Resonance Imaging Substudy. Stroke 2013;44:80-6.
6. Bonati LH, Jongen LM, Haller S, Flach HZ, Dobson J, Nederkoorn PJ, et al. New ischaemic brain lesions on MRI after stenting or endarterectomy for symptomatic carotid stenosis: a substudy of the International Carotid Stenting Study (ICSS). Lancet Neurol 2010;9:353-62.
7. Hammer FD, Lacroix V, Duprez T, Grandin C, Verhelst R, Peeters A, et al. Cerebral microembolization after protected carotid artery stenting in surgical high-risk patients: results of a 2-year prospective study. J Vasc Surg 2005;42:847-53.
8. Stabile E, Sannino A, Schiattarella GG, Gargiulo G, Toscano E, Brevetti L, et al. Cerebral embolic lesions detected with diffusion-weighted magnetic resonance imaging following carotid artery stenting: a meta-analysis of 8 studies comparing filter cerebral protection and proximal balloon occlusion. JACC Cardiovasc Interv 2014;7:1177-83.
9. Bijuklic K, Wandler A, Varnakov Y, Tuebler T, Schofer J. Risk factors for cerebral embolization after carotid artery stenting with embolic protection a diffusion-weighted magnetic resonance imaging study in 837 consecutive patients. Circ Cardiovasc Interv 2013;6:311-6.
10. Bijuklic K, Wandler A, Hazizi F, Schofer J. The PROFI study (Prevention of Cerebral Embolization by Proximal Balloon Occlusion Compared to Filter Protection During Carotid Artery Stenting): a prospective randomized trial. J Am Coll Cardiol 2012;59:1383-9.
11. Montorsi P, Caputi L, Galli S, Ciceri E, Ballerini G, Agrifoglio M, et al. Microembolization during carotid artery stenting in patients with high-risk, lipid-rich plaque: a randomized trial of proximal versus distal cerebral protection. J Am Coll Cardiol 2011;58:1656-63.
12. Antonius CE. Transcranial Doppler monitoring in angioplasty and stenting of the carotid bifurcation. J Endovasc Ther 2003;10:702.
13. Kim H, Lee H, Yang J, Yeo I, Yi J, Lee I, et al. The influence of carotid artery catheterization technique on the incidence of thromboembolism during carotid artery stenting. AJNR Am J Neuroradiol 2010;31:1732-6.
14. Verzini F, Cao P, De Rango P, Parlani G, Maselli A, Romano L, et al. Appropriateness of learning curve for carotid artery stenting: an analysis of periprocedural complications. J Vasc Surg 2006;44:1205-11.
15. Kahlert P, Knipp SC, Schlamann M, Thielmann M, Al-Rashid F, Weber M, et al. Silent and apparent cerebral ischemia after percutaneous transfemoral aortic valve implantation: a diffusion-weighted magnetic resonance imaging study. Circulation 2010;121:870-8.
16. Smith CR, Leon MB, Mack MJ, Miller DC, Moses JW, Svensson LG, et al. Transcatheter versus surgical aortic-valve replacement in high-risk patients. N Engl J Med 2011;364:2187-98.
17. Omran H, Schmidt H, Hackenbroch M, Illien S, Bernhardt P, von der Recke G, et al. Silent and apparent cerebral embolism after retrograde catheterisation of the aortic valve in valvular stenosis: a prospective, randomised study. Lancet 2003;361:1241-6.
18. Bismuth J, Garami Z, Anaya-Ayala JE, Naoum JJ, El Sayed HF, Peden EK, et al. Transcranial Doppler findings during thoracic endovascular aortic repair. J Vasc Surg 2011;54:364-9.
19. Yokoyama K, Nakagawa H, Shah DC, Lambert H, Leo G, Aeby N, et al. Novel contact force sensor incorporated in irrigated radiofrequency ablation catheter predicts lesion size and incidence of steam pop and thrombus. Circ Arrhythm Electrophysiol 2008;1:354-62.
20. Natale A, Reddy VY, Monir G, Wilber DJ, Lindsay BD, McElderry HT, et al. Paroxysmal AF catheter ablation with a contact force sensing catheter: results of the prospective, multicenter SMART-AF trial. J Am Coll Cardiol 2014;64:647-56.
21. Pinter L, Ribo M, Loh C, Lane B, Roberts T, Chou TM, et al. Safety and feasibility of a novel transcervical access neuroprotection system for carotid artery stenting in the PROOF Study. J Vasc Surg 2011;54:1317-23.
22. Leal I, Orgaz A, Flores Á, Gil J, Rodríguez R, Peinado J, et al. A diffusion-weighted magnetic resonance imaging-based study of transcervical carotid stenting with flow reversal versus transfemoral filter protection. J Vasc Surg 2012;56:1585-90.
23. Rafii-Tari H, Payne CJ, Yang GZ. Current and emerging robot-assisted endovascular catheterization technologies: a review. Ann Biomed Eng 2014;42:697-715.
24. Bonatti J, Vetrovec G, Riga C, Wazni O, Stadler P. Robotic technology in cardiovascular medicine. Nat Rev Cardiol 2014;11: 266-75.
25. Riga CV, Bicknell CD, Hamady MS, Cheshire NJ. Evaluation of robotic endovascular catheters for arch vessel cannulation. J Vasc Surg 2011;54:799-809.
26. Riga C, Rolls A, Rippel R, Shah C, Hamady M, Bicknell C, et al. Advantages and limitations of robotic endovacular catheters for carotid artery stenting. J Cardiovasc Surg 2012;53:747-53.
27. Riga CV, Bicknell CD, Rolls A, Cheshire NJ, Hamady MS. Robot-assisted fenestrated endovascular aneurysm repair (FEVAR) using the Magellan System. J Vasc Interv Radiol 2013;24:191-6.
28. Bai R, Di Biase L, Valderrabano M, Lorgat F, Mlcochova H, Tilz R, et al. Worldwide experience with the robotic navigation system in catheter ablation of atrial fibrillation: methodology, efficacy and safety. J Cardiovasc Electrophysiol 2012;23:820-6.
29. Rolls AE, Riga CV, Bicknell CD, Regan L, Cheshire NJ, Hamady MS. Robot-assisted uterine artery embolization: a first-in-woman safety evaluation of the Magellan System. J Vasc Interv Radiol 2014;25: 1841-8.
30. Bismuth J, Duran C, Stankovic M, Gersak B, Lumsden AB. A first-in-man study of the role of flexible robotics in overcoming navigation challenges in the iliofemoral arteries. J Vasc Surg 2013;57:14S-9S.
31. de Ruiter QM, Moll FL, van Herwaarden JA. Current state in tracking and robotic navigation systems for application in endovascular aortic aneurysm repair. J Vasc Surg 2015;61:256-64.
32. Shah C, Riga C, Stoyanov D, Rolls A, Van Herzeele I, Yang G, et al. Video motion analysis for objective assessment in catheter-based endovascular intervention. Br J Surg 2012;99:1-16.
33. Bismuth J, Kashef E, Cheshire N, Lumsden AB. Feasibility and safety of remote endovascular catheter navigation in a porcine model. J Endovasc Ther 2011;18:243-9.
34. Duran C, Lumsden AB, Bismuth J. A randomized, controlled animal trial demonstrating the feasibility and safety of the Magellan endovascular robotic system. Ann Vasc Surg 2014;28:470-8.
35. Reiley CE, Akinbiyi T, Burschka D, Chang DC, Okamura AM, Yuh DD. Effects of visual force feedback on robot-assisted surgical task performance. J Thorac Cardiovasc Surg 2008;135:196-202.
36. Horeman T, Rodrigues SP, Jansen FW, Dankelman J, van den Dobbelsteen JJ. Force parameters for skills assessment in laparoscopy. IEEE Trans Haptics 2012;5:312-22.
37. Reddy VY, Shah D, Kautzner J, Schmidt B, Saoudi N, Herrera C, et al. The relationship between contact force and clinical outcome during radiofrequency catheter ablation of atrial fibrillation in the TOCCATA study. Heart Rhythm 2012;9:1789-95.
38. Neuzil P, Reddy VY, Kautzner J, Petru J, Wichterle D, Shah D, et al. Electrical reconnection after pulmonary vein isolation is contingent on contact force during initial treatment results from the EFFICAS I study. Circ Arrhythm Electrophysiol 2013;6:327-33.
39. Okumura Y, Johnson SB, Bunch TJ, Henz BD, O'Brien CJ, Packer DL. A systematical analysis of in vivo contact forces on virtual catheter tip/tissue surface contact during cardiac mapping and intervention. J Cardiovasc Electrophysiol 2008;19:632-40.
40. Rafii-Taril H, Payne CJ, Riga C, Bicknell C, Lee SL, Yang GZ. Assessment of navigation cues with proximal force sensing during endovascular catheterization. Med Image Comput Comput Assist Interv 2012;15(Pt 2):560-7.
41. Payne CJ, Rafii-Tari H, Yang GZ. A force feedback system for endovascular catheterisation. IEEE/RSJ International Conference on Intelligent Robots and Systems; 2012:1298-304.
42. Lin PH, Bush RL, Peden EK, Zhou W, Guerrero M, Henao EA, et al. Carotid artery stenting with neuroprotection: assessing the learning curve and treatment outcome. Am J Surg 2005;190:855-63.
43. Riga C, Bicknell C, Sidhu R, Cochennec F, Normahani P, Chadha P, et al. Advanced catheter technology: is this the answer to overcoming the long learning curve in complex endovascular procedures? Eur J Vasc Endovasc Surg 2011;42:531-8.

44. Neequaye SK, Aggarwal R, Van Herzeele I, Darzi A, Cheshire NJ. Endovascular skills training and assessment. J Vasc Surg 2007;46:1055-64.
45. Tedesco MM, Pak JJ, Harris EJ Jr, Krummel TM, Dalman RL, Lee JT. Simulation-based endovascular skills assessment: the future of credentialing? J Vasc Surg 2008;47:1008-14.
46. Rolls AE, Riga CV, Bicknell CD, Stoyanov DV, Shah CV, Van Herzeele I, et al. A pilot study of video-motion analysis in endovascular surgery: development of real-time discriminatory skill metrics. Eur J Vasc Endovasc Surg 2013;45:509-15.
47. Coles T, Meglan D, John N. The role of haptics in medical training simulators: a survey of the state-of-the-art. IEEE Trans Haptics 2011;4:51-66.
48. Rafii-Tari H, Payne CJ, Liu J, Riga C, Bicknell C, Yang GZ. Towards automated surgical skill evaluation of endovascular catheterization tasks based on force and motion signatures. IEEE Int Conf Robot Autom 2015:1789-94.
49. Rippel RA, Rolls AE, Riga CV, Hamady M, Cheshire NJ, Bicknell CD. The use of robotic endovascular catheters in the facilitation of transcatheter aortic valve implantation. Eur J Cardiothorac Surg 2014;45:836-41.

Submitted Apr 14, 2015; accepted Jun 16, 2015.